Nuclear Instruments and Methods in Physics Research A290 (1990) 335–345
North-Holland

EXPERIMENTAL DETERMINATION OF SAMPLING FLUCTUATIONS IN URANIUM AND LEAD HADRONIC CALORIMETERS

G. DREWS [1], M.A. GARCIA [2]*, R. KLANNER [1], U. KÖTZ [1], M. KRÄMER [3]**, J. DEL PESO [2]*, E. ROS [1], F. SELONKE [1], J. STRAVER [4], H. TIECKE [4] and M. TSIROU [5]+

[1] *DESY, D-2000 Hamburg 52, FRG*
[2] *Univ. Autónoma de Madrid, 28049 Madrid, Spain*
[3] *Univ. of Bonn, 5300 Bonn, FRG*
[4] *NIKHEF-H, 1009 DB Amsterdam, The Netherlands*
[5] *Univ. of Wisconsin, Madison, WI 53706, USA*

Received 28 December 1989

We study the energy resolution of two compensating sandwich calorimeters using scintillators as readout material and lead and uranium as absorber, respectively. By employing the technique of the two interleaved calorimeters we extract the contribution of sampling and intrinsic fluctuations. We find that the energy resolution for hadrons is dominated by sampling fluctuations in both cases.

1. Introduction

Hadron sampling calorimeters have attracted considerable interest in the last years. This interest can be explained on one side by the physics goals to be achieved at high-energy colliders (Tevatron, HERA, LHC, SSC) and on the other side by the progress in understanding the basic phenomena involved in hadronic cascades. The concept of "compensation" (equal response to electrons and hadrons) has been clarified both by Monte Carlo calculations and by several recent experimental measurements. Detailed Monte Carlo calculations [1–3] have shown the importance of detecting the low-energy neutron component of the hadron shower in order to achieve compensation and therefore the advantage of readout media containing a large fraction of hydrogen like scintillators. Experimentally, compensation has been obtained with calorimeters using uranium [4,6] or lead [5] as absorber material and plastic scintillator or gas for the readout.

The present developments in the field of hadron calorimetry follow two directions:

1) obtaining compensation with other readout media than scintillator or gas, like liquid argon [7], TMP [8] or silicon [9],
2) improving the energy resolution of hadron calorimeters which are known to be compensating, like lead–scintillator calorimeters. The field of "precise hadron calorimetry" has emerged in this way and the best example of development is the so-called "spaghetti calorimeter" [10].

Progress in the second line of research requires a detailed understanding of the energy fluctuations inside hadronic cascades. This paper is an attempt to determine experimentally the different contributions to these fluctuations [++].

2. Energy resolution of sampling calorimeters

A sandwich calorimeter (see fig. 1) consists of absorber plates, generally made of a high-Z material, separated by gaps where the active medium (or readout medium) is located. The sampling ratio R is the ratio

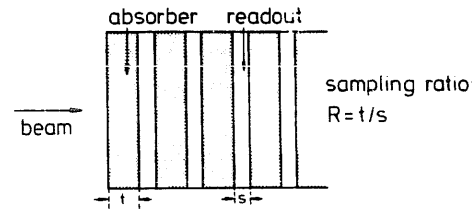

Fig. 1. A sampling calorimeter with absorber thickness t, readout material thickness s and sampling ratio R.

* Supported by DAAD.
** Supported by BMFT.
\+ Supported by DOE.

[++] A preliminary version of the results presented here can be found in ref. [11].

between the thickness of the absorber, t, and the thickness of the active medium, s: $R = t/s$.

The response of sandwich calorimeters to electromagnetic showers is well known from both the experimental and the Monte Carlo points of view. We have the following relation:

$$E_{\text{vis}} = eE,$$

where E and E_{vis} are, respectively, the energy of the showering particle and the visible energy in the readout medium. The parameter e is the electromagnetic sampling fraction and is usually referred to the sampling fraction of a "mip" (minimum ionizing particle):

$$\text{mip} = \frac{(\mathrm{d}E/\mathrm{d}x)_s}{(\mathrm{d}E/\mathrm{d}x)_s + R(\mathrm{d}E/\mathrm{d}x)_t},$$

where $(\mathrm{d}E/\mathrm{d}x)_s$ and $(\mathrm{d}E/\mathrm{d}x)_t$ are the minimum ionizing losses per unit length of active medium or absorber, respectively. The ratio e/mip depends almost exclusively on the difference in charge number Z between the absorber and the readout medium, decreasing as the difference in Z increases (transition effect). Typical e/mip ratios for heavy absorbers and light readout media are between 0.6 and 0.7 [3].

The energy resolution of electromagnetic calorimeters is

$$\frac{\Delta E_{\text{vis}}}{E_{\text{vis}}} = \frac{\Delta e}{e} = \frac{a}{\sqrt{E}} \quad (E \text{ in GeV}),$$

where all experimental data indicate that the parameter a is energy-independent and approximately proportional to $\sqrt{t}$. The following parametrization has been proposed [12]:

$$a = 3.2\%\sqrt{\Delta\epsilon[\text{MeV}]} \quad \text{with} \quad \Delta\epsilon = t\left(\frac{\mathrm{d}E}{\mathrm{d}x}\right)_t + s\left(\frac{\mathrm{d}E}{\mathrm{d}x}\right)_s.$$

The response of sampling calorimeters to hadron showers is more complex and not so well studied. The sampling fraction h is again defined as

$$E_{\text{vis}} = hE.$$

The energy of the shower splits in the following components:

$$E = E_{\text{em}} + E_{\pi} + E_{\text{p}} + E_{\text{n}} + E_{\text{Nucl}},$$

where E_{em} is the electromagnetic component (mainly produced by π^0), E_{π} the charged pion one, E_{p} the proton one, E_{n} the neutron one and finally E_{Nucl} is the energy lost in breaking the nuclear binding energy (sometimes called "invisible energy") or taken by nuclear fragments. Each component has its own sampling fraction *, therefore,

$$E_{\text{vis}} = eE_{\text{em}} + \pi E_{\pi} + pE_{\text{p}} + nE_{\text{n}} + NE_{\text{Nucl}},$$

* The detection efficiency of the readout medium for the different components plays also an important role in hadron showers and has to be included in the sampling fraction.

where the sampling fraction for the nuclear component, N, is normally a vanishing quantity. As a result e/h is larger than 1 for typical noncompensating hadron calorimeters. As commented before, e/mip is almost independent of R and the same occurs for π/mip and p/mip since charged hadrons are very similar to minimum ionizing particles. This is not the case for low energy neutrons: Monte Carlo calculations show that n/mip is approximately proportional to R [3] and therefore e/h can be tuned by varying R [2]. It has been shown experimentally that for calorimeters with enough neutron yield (mainly uranium, but also lead calorimeters) and a significant neutron sampling fraction (scintillator calorimeters, for example), values of e/h close to 1 (compensation) or even smaller than 1 (overcompensation) can be achieved.

The fluctuations of the visible energy have two different origins in hadron showers:

- the fluctuations of the sampling fractions (Δe, $\Delta\pi$, etc.), which produce "sampling fluctuations" as for electromagnetic showers and can be reduced by reducing the sampling step,
- the fluctuations of the shower components (ΔE_{em}, ΔE_{π}, etc.) which, through the different sampling fractions, produce the so-called "intrinsic fluctuations".

This suggests the following empirical formula for the fractional energy resolution of hadron calorimeters:

$$\frac{\Delta E_{\text{vis}}}{E_{\text{vis}}} = \frac{\Delta h}{h} = \sigma_{\text{samp}} \oplus \sigma_{\text{intr}},$$

where σ_{samp} is a function of $\sqrt{t}$ (as for the electromagnetic case) and σ_{intr} is a function of R (note that σ_{intr} depends on the sampling fractions). In ref. [12], the following parametrization based on experimental data has been proposed for the sampling fluctuations:

$$\sigma_{\text{samp}} = \frac{a}{\sqrt{E}} \quad (E \text{ in GeV}),$$

with

$$a = 9.0\%\sqrt{\Delta\epsilon[\text{MeV}]}.$$

The energy dependence of σ_{intr} is more complicated. Both experimental and Monte Carlo information indicate that σ_{intr} does not scale with $\sqrt{E}$. A successful parametrization is (see ref. [3] for details):

$$\sigma_{\text{intr}} = \frac{b}{\sqrt{E}} + c,$$

where c depends on the e/h ratio, vanishing for compensating calorimeters. According to all these assumptions, both σ_{samp} and σ_{intr} scale with $\sqrt{E}$ for compensating calorimeters, and therefore, the fractional energy resolution as well. This result is supported by all existing experimental data [4–6].

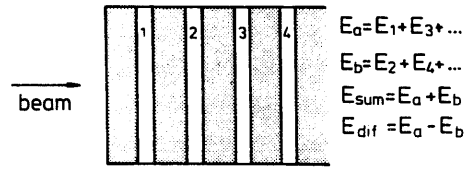

Fig. 2. The two interleaved calorimeters with the definitions of of E_a, E_b (partial energy sums), E_{sum} (total energy) and E_{dif} (energy difference).

3. Experimental determination of sampling fluctuations

In order to extract sampling fluctuations from the total fluctuations in hadronic calorimeters, we have used the technique of the "two interleaved calorimeters". This technique was already employed long time ago for the case of liquid argon calorimeters [13].

The two interleaved calorimeters are shown in fig. 2. They result from summing up odd-number readout layers (calorimeter a) and even-number readout layers (calorimeter b). These two calorimeters can be regarded as two independent sampling calorimeters embedded in the original one. It is useful to define the following relative fluctuations:

$$\sigma_a = \frac{\Delta E_a}{\langle E_a \rangle}, \quad \sigma_b = \frac{\Delta E_b}{\langle E_b \rangle},$$

$$\sigma_{sum} = \frac{\Delta E_{sum}}{\langle E_{sum} \rangle}, \quad \sigma_{dif} = \frac{\Delta E_{dif}}{\langle E_{sum} \rangle},$$

where $\langle E_a \rangle$ and $\langle E_b \rangle$ are the average energy sums measured by the two calorimeters, $\langle E_{sum} \rangle = \langle E_a + E_b \rangle$, $\langle E_{dif} \rangle = \langle E_a - E_b \rangle$ their sum and difference, and finally ΔE_a, ΔE_b, ΔE_{sum} and ΔE_{dif} are the corresponding fluctuations. The resolution of the complete calorimeter is obtained by summing the two calorimeters and the decrease in resolution due to the coarser sampling is obtained from the fluctuations of the two partial sums (σ_a and σ_b) or better, from the fluctuations in their difference (σ_{dif}).

The way this technique works is more easily understood in the electromagnetic case. Since in this case only sampling fluctuations are present and the absorber thickness of the two interleaved calorimeters is $2t$, we expect

$$\sigma_{sum} = \sigma_{samp} \quad \text{and} \quad \sigma_a = \sigma_b = \sqrt{2}\,\sigma_{samp}.$$

where σ_{samp} are the sampling fluctuations for the complete calorimeter. Since the sampling fluctuations for calorimeters a and b are independent:

$$\Delta E_{sum} = \Delta E_{dif},$$

and therefore

$$\sigma_{dif} = \sigma_{sum}.$$

These equations can of course be checked using the Monte Carlo shower generator EGS4 [14]. We have simulated the response of a calorimeter consisting of 10 mm thick lead plates sandwiched with 2.5 mm thick scintillator plates to electrons in the energy range between 1 and 20 GeV. The values obtained for σ_{sum}, σ_{dif}, σ_a and σ_b are shown in table 1. we note that, as expected, all these quantities scale with $\sqrt{E}$, that $\sigma_{sum} \approx \sigma_{dif}$ and finally that $\sigma_a \approx \sigma_b \approx \sqrt{2}\,\sigma_{sum}$. In fact σ_{dif} is slightly larger than σ_{sum} (by about 10%), and this is due to a small negative correlation between the energies deposited in calorimeters a and b. The correlation coefficient, defined in the usual way,

$$\sigma_{ab} = \frac{\langle (E_a - \langle E_a \rangle)(E_b - \langle E_b \rangle) \rangle}{\sigma_a \sigma_b} \quad (-1 < \sigma_{ab} < 1),$$

is also included in table 1. The energies E_a and E_b are also shown in a correlation plot in fig. 3 for $E = 10$ GeV, no significant correlation being observed.

As explained in the previous section, hadronic showers have intrinsic fuctuations in addition to the sampling ones. These intrinsic fluctuations are produced by fluctuations between the different shower components. On an event-by-event base, these fluctuations are the same for calorimeters a and b, and the complete calorimeter as well. Due to this important property of the two interleaved calorimeters, the intrinsic fluctuations contribute in the same way to σ_a, σ_b and σ_{sum}, but cancel when σ_{dif} is considered. The sampling fluctuations, on the other side, can be considered as independent for calorimeters a and b, as for electro-

Table 1
Energy fluctuations as simulated by EGS4 for 1, 5, 10 and 20 GeV electron showers entering a Pb (10 mm) scintillator (2.5 mm) sampling calorimeter

	$E = 1$ GeV	5 GeV	10 GeV	20 GeV
$\sigma_{sum}\sqrt{E}$ [%]	23.8 ±1.0	22.3 ±0.9	23.2 ±0.9	21.9 ±0.9
$\sigma_{dif}\sqrt{E}$ [%]	24.7 ±1.0	27.6 ±1.2	25.3 ±1.0	25.8 ±1.1
$\sigma_a\sqrt{E}$ [%]	33.0 ±1.3	34.1 ±1.5	35.3 ±1.3	32.6 ±1.4
$\sigma_b\sqrt{E}$ [%]	35.7 ±1.4	36.8 ±1.6	33.3 ±1.0	34.8 ±1.4
σ_{ab}	−0.04±0.08	−0.22±0.08	−0.09±0.08	−0.17±0.08

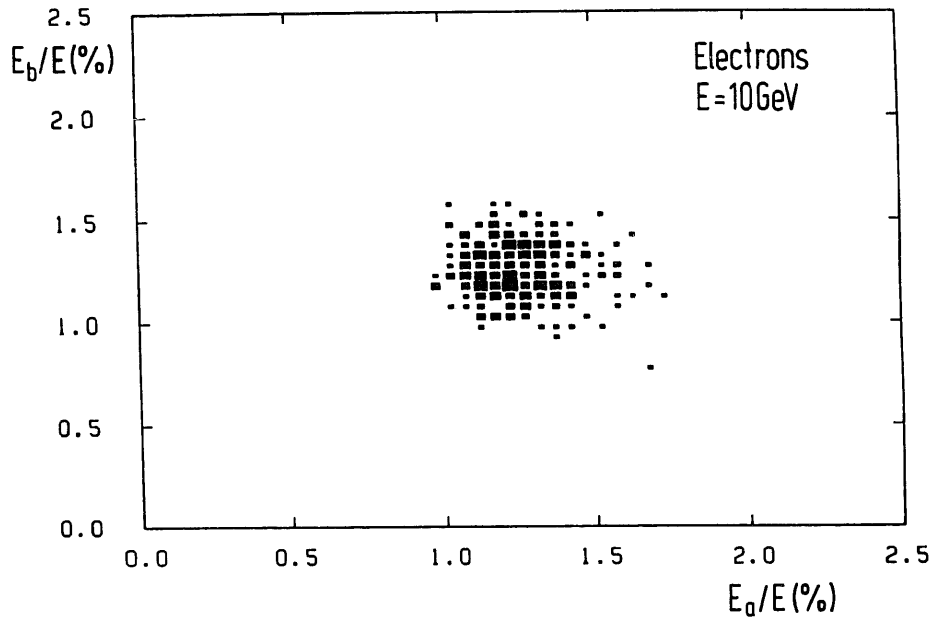

Fig. 3. Correlation plot for the energy fractions deposited in the active material of two interleaved calorimeters as simulated by EGS4 for 10 GeV electron showers. The complete calorimeter consists of lead (10 mm sampling) and scintillator (2.5 mm sampling).

magnetic showers. We have therefore the following relations for hadronic calorimeters:

$\sigma_{sum} = \sigma_{int} \oplus \sigma_{samp}$,

$\sigma_a = \sigma_b = \sigma_{int} \oplus \sqrt{2}\,\sigma_{samp}$,

$\sigma_{dif} = \sigma_{samp}$.

We note that the e/h ratio for calorimeters a and b is the same as for the complete calorimeter and that these equations hold both for compensating and for noncompensating calorimeters. We apply them in the following to compensating calorimeters using scintillator as the readout material. This implies a modification of the equations due to instrumental effects. This modifications will be discussed in section 7.

4. Description of the calorimeters

We have performed our measurements with a lead–scintillator and a uranium–scintillator calorimeter. These calorimeters were built to investigate compensation and energy resolution for lead and uranium as absorbers and have already been described in detail in refs. [5] and [6], respectively. We give here only a brief summary for completeness.

The lead calorimeter (see fig. 4) was a sandwich of 10 mm thick lead plates and 2.5 mm thick scintillator plates. The ratio of 4 between lead and scintillator thicknesses was optimized to achieve compensation according to Monte Carlo predictions. The calorimeter consisted of 9 towers, 20×20 cm^2 each, so the total cross section perpendicular to the beam was about 60×60 cm^2. Longitudinally each tower was segmented in an EMC section (1λ or $29X_0$ deep) and a HAD section (4λ deep). Each section was read out on the right and the left side by PMs (XP2011 type from Philips) via wavelength shifter plates (WLS) and light guides. The scintillator material used was SCSN-38 and the WLS plates were made of PMMA doped with K-27 in a concentration of 125 mg/l. The uniformity of light collection along the WLS plates was optimized with graded filters adjusted according to bench test measurements.

The uranium calorimeter consisted of four separate but identical modules (see fig. 5). Each module contained 45 layers of 3.2 mm thick uranium and 3.0 mm thick scintillator plates. The total cross section perpendicular to the beam was 60×60 cm^2. In the vertical direction the scintillator plane was segmented into 12 strips, 5 cm high, in order to provide information on the lateral development of the shower. The light from each strip was transmitted to PMs via wavelength shifter bars and plexiglas light guides. These light guides were bent such that two modules could approach each other without leaving any significant dead space between them. Graded filters were also introduced between the scintillator and the WLS to compensate for the attenuation along the WLS material. The optical materials and the PM type were the same as for the lead calorimeter.

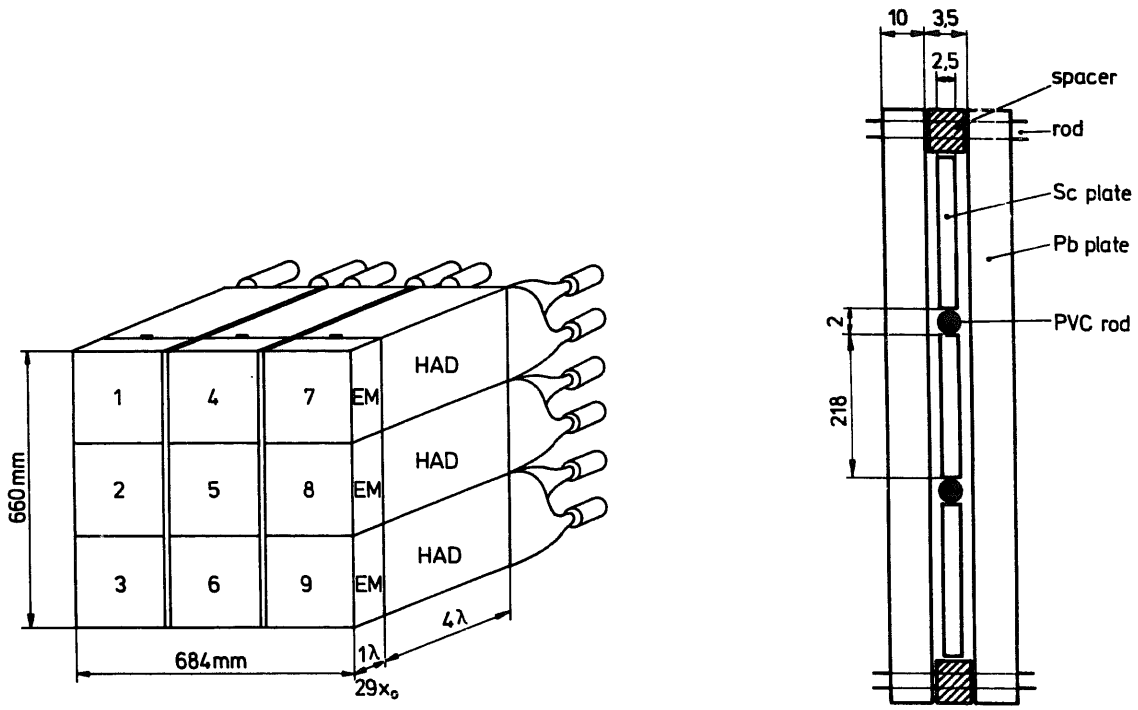

Fig. 4. The lead–scintillator calorimeter with a detail of the layer structure.

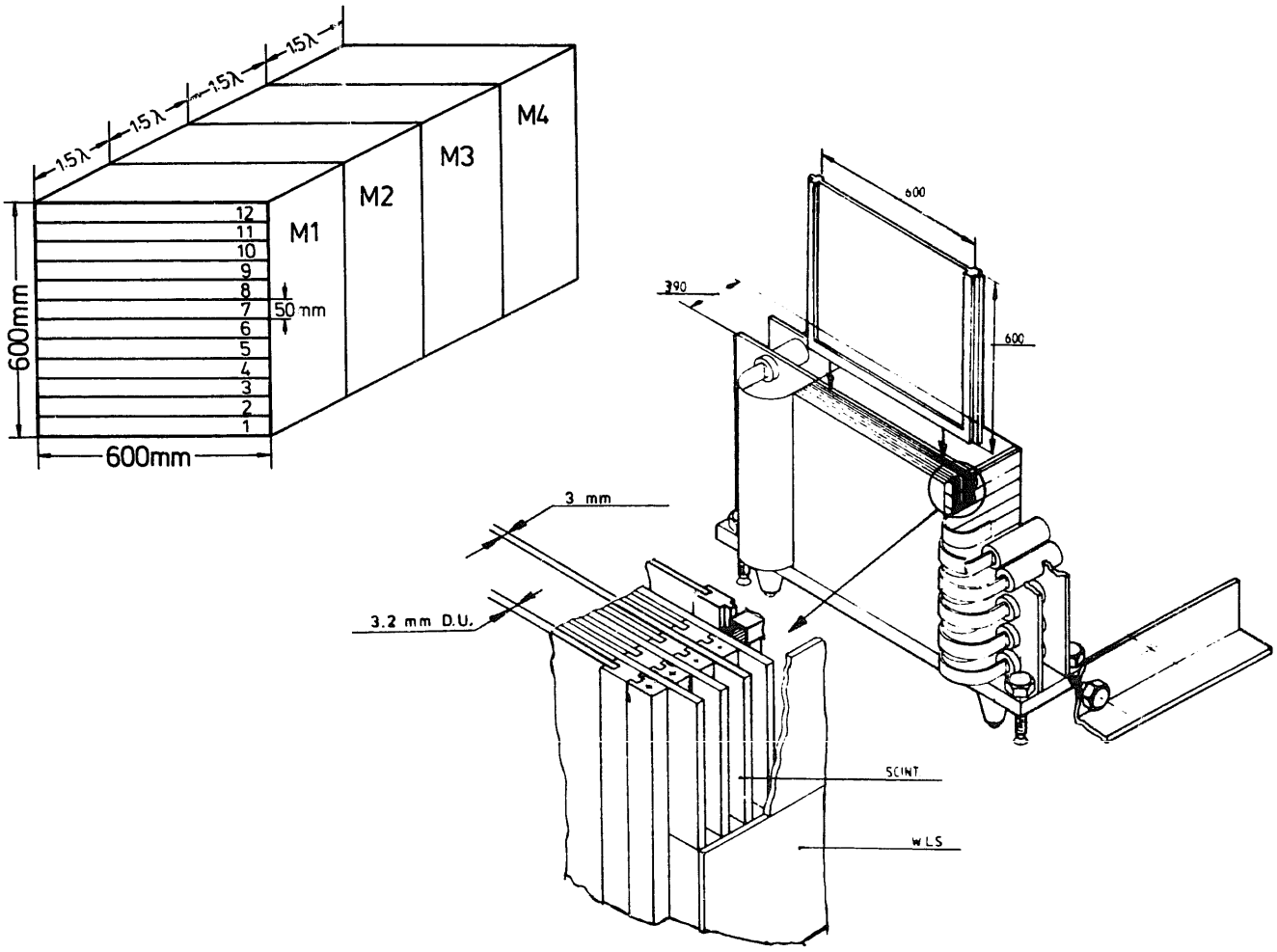

Fig. 5. The uranium–scintillator calorimeter with a detail of the layer structure.

Table 2
Calorimeter parameters

	Pb calorimeter	DU calorimeter
Absorber material	Pb (4% Sb)	depleted U
Scintillator material	SCSN-38	SCSN-38
WLS material	PMM UV absorbant doped with K27 (125 mg/l)	PMM UV absorbant doped with K27 (120 mg/l)
Photomultipliers	Philips XP2011	Philips XP2011
Absorber thickness	10 mm	3.2 mm
Scintillator thickness	2.5 mm	3.0 mm
Lateral segmentation	20×20 cm^2 (9 towers)	5×60 cm^2 (12 strips)
Calorimeter cross section	60×60 cm^2	60×60 cm^2
Longitudinal segmentation	EMC(1λ)+ HAC(4λ)	4 modules (1.5λ)
Calorimeter depth	5λ	6λ
Number of readout channels	36	96

The main parameters of both calorimeters are reported in table 2.

5. Experimental setup and calibration

The calorimeters were tested in the X5 test beam of the CERN-SPS, in the energy range between 10 and 50 GeV. We estimate the momentum spread of this beam to be less than 1% for the collimator settings used during the measurements. The modules were installed on a support allowing both horizontal and vertical movements. The measurements were performed with positively charged particles.

The beam was defined by a pair of scintillation counters, B1 and B2 (see fig. 6). A veto counter, B3, with 1 cm diameter hole in the middle, was used to reject beam halo particles. Electron-to-hadron separation was provided by two Cherenkov counters, C1 and C2, filled with helium and nitrogen, respectively. The second counter, C2, was used in the trigger. A

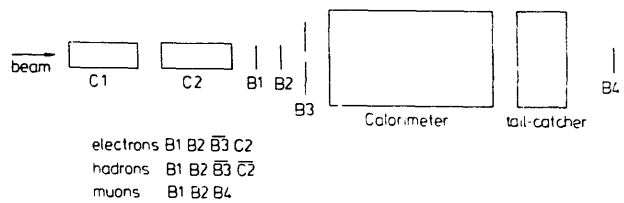

Fig. 6. Experimental setup in the beamline and typical trigger conditions.

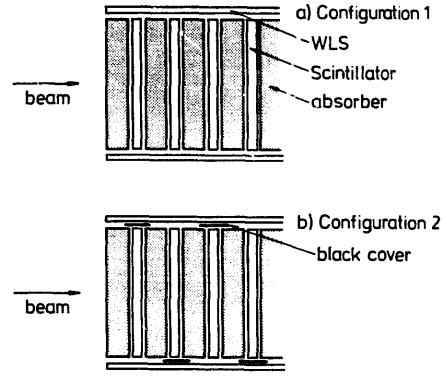

Fig. 7. Calorimeter setups used in the test: (a) all plates are read out on both sides (configuration 1); (b) each plate is read out only on one side (configuration 2).

uranium–scintillator calorimeter module, 1λ deep, was used as tail catcher for both calorimeters. Finally an additional scintillator counter, B4, located behind the calorimeters was used to trigger on muons.

The photomultiplier signals were digitized by LeCroy 2282B ADCs of 12 bits, with integration gates of 150 ns, and read out by front-end microprocessors (Texas TMS-99010) using a PDP11 as host computer.

The measurements reported in refs. [5] and [6] were performed with a calorimeter configuration where all scintillator plates are read out (configuration 1 in fig. 7). The measurements reported here were performed with a configuration where the WLS plates situated on one side could only read the scintillator plates with even number and those on the other side the scintillator plates with odd number (configuration 2 in fig. 7). This was achieved by covering the corresponding readout side of each scintillator plate with black tape. In the case of the lead calorimeter, a piece of teflon was inserted between the black tape and the scintillator in order not to loose in light yield. By summing both sides of the calorimeter the complete readout is recovered, whereas by considering the individual sides or the difference in response, event by event, sampling fluctuations can be measured as discussed in section 3.

The calibration procedures have been described in detail, for the case of configuration 1, in refs. [5] and [6]. They were applied for the case of configuration 2 as well. We briefly summarize them below.

1) Lead calorimeter: the center of each tower was exposed to 50 GeV electrons, hadrons and muons. The calibration constants were obtained by balancing the response to electrons of each EMC channel and the response to hadrons of each HAC channel. The muon signal was used for cross-checks and to intercalibrate EMC and HAC sections.
2) Uranium calorimeter: the uranium radioactivity, integrated with a 10000 ns long gate, provided a calibration of all calorimeter channels within 3%

accuracy. In order to improve this calibration, the front module was also exposed to 50 GeV electron beams incident at the center of each strip. Muons and hadrons were also used for cross-checks.

6. The data

Both calorimeters were exposed to electrons and hadrons in the energy range between 10 and 50 GeV for configuration 1 (standard readout) and 2 (interleaved calorimeters). The event selection criteria and treatment of the data are as in refs. [5] and [6]. The results obtained for configuration 1 have been published there, so only the values relevant for the present analysis are reported here.

The results obtained for the lead calorimeter are reported in tables 3a (configuration 1) and 3b (configuration 2). The results of the uranium calorimeter are

Table 3a
Results from the lead calorimeter (configuration 1)

E [GeV]	Hadrons			Electrons			e/h
	$\sigma_{sum}\sqrt{E}$ [%]	$\sigma_{dif}\sqrt{E}$ [%]	$\sigma_{side}\sqrt{E}$ [%]	$\sigma_{sum}\sqrt{E}$ [%]	$\sigma_{dif}\sqrt{E}$ [%]	$\sigma_{side}\sqrt{E}$ [%]	
10	45.6±0.7	10.5±0.2	47.1±0.5	24.2±0.4	8.4±0.2	25.5±0.3	1.12±0.01
20	42.0±0.7	10.1±0.2	42.8±0.5	23.9±0.5	8.3±0.2	25.4±0.3	1.11±0.01
30	43.7±0.7	10.2±0.2	45.0±0.5	24.3±0.5	8.6±0.2	25.8±0.3	1.10±0.01
50	42.5±0.7	10.5±0.2	44.1±0.5	25.1±0.6	9.2±0.2	26.5±0.4	1.10±0.01
Average	43.5±1.0	10.3±1.0	44.8±1.0	24.4±1.0	8.6±1.0	25.8±1.0	

Table 3b
Results from the lead calorimeter (configuration 2)

E [GeV]	Hadrons			Electrons			e/h
	$\sigma_{sum}\sqrt{E}$ [%]	$\sigma_{dif}\sqrt{E}$ [%]	$\sigma_{side}\sqrt{E}$ [%]	$\sigma_{sum}\sqrt{E}$ [%]	$\sigma_{dif}\sqrt{E}$ [%]	$\sigma_{side}\sqrt{E}$ [%]	
10	43.8±0.6	40.7±0.3	59.5±1.0	23.7±0.3	25.8±0.3	35.1±0.3	1.13±0.01
20	43.8±0.6	43.5±0.3	60.2±1.0	24.5±0.3	26.5±0.3	36.0±0.6	1.12±0.01
30	42.4±0.6	42.7±0.3	61.6±1.0	24.7±0.3	26.7±0.3	36.3±0.6	1.11±0.01
50	43.9±0.6	42.4±0.3	60.6±1.0	24.9±0.3	27.1±0.3	36.8±0.6	1.10±0.01
Average	43.5±1.0	42.3±1.0	60.5±1.0	24.5±1.0	25.8±1.0	36.0±1.0	

Table 4a
Results from the uranium calorimeter (configuration 1)

E [GeV]	Hadrons			Electrons			e/h
	$\sigma_{sum}\sqrt{E}$ [%]	$\sigma_{dif}\sqrt{E}$ [%]	$\sigma_{side}\sqrt{E}$ [%]	$\sigma_{sum}\sqrt{E}$ [%]	$\sigma_{dif}\sqrt{E}$ [%]	$\sigma_{side}\sqrt{E}$ [%]	
10	35.8±0.7	10.5±0.2	37.6±0.5	17.3±0.4	8.1±0.2	19.4±0.3	1.01±0.01
20	34.4±0.7	11.7±0.2	36.4±0.5	16.4±0.5	8.0±0.2	18.3±0.3	1.01±0.01
30	35.6±0.7	12.0±0.2	37.6±0.5	17.0±0.5	6.2±0.2	18.1±0.3	1.02±0.01
50	37.5±0.7	12.7±0.2	39.3±0.5	17.7±0.6	8.6±0.2	19.8±0.4	1.02±0.01
Average	35.8±1.0	11.7±1.0	37.7±1.0	17.1±1.0	8.2±1.0	18.9±1.0	

Table 4b
Results from the uranium calorimeter (configuration 2)

E [GeV]	Hadrons			Electrons			e/h
	$\sigma_{sum}\sqrt{E}$ [%]	$\sigma_{dif}\sqrt{E}$ [%]	$\sigma_{side}\sqrt{E}$ [%]	$\sigma_{sum}\sqrt{E}$ [%]	$\sigma_{dif}\sqrt{E}$ [%]	$\sigma_{side}\sqrt{E}$ [%]	
10	38.8±0.6	28.7±0.3	48.3±1.0	18.2±0.3	18.3±0.3	25.6±0.6	1.00±0.01
20	36.5±0.6	34.6±0.3	49.5±1.0	18.2±0.3	19.6±0.3	27.0±0.6	1.00±0.01
30	36.4±0.6	33.9±0.3	50.1±1.0	18.6±0.3	19.4±0.3	27.0±0.6	1.00±0.01
50	37.4±0.6	33.2±0.3	50.0±1.0	19.0±0.3	19.7±0.3	27.5±0.6	1.00±0.01
Average	37.3±1.0	32.6±1.0	49.5±1.0	18.5±1.0	19.2±1.0	26.8±1.0	

reported in tables 4a (configuration 1) and 4b (configuration 2). The errors indicated in these tables are the statistical errors for each energy point and the estimated total error for the averages. For both configurations, a readout on the left and the right side of the different calorimeter sections was available. We define the quantity

$$\sigma_{side} = \tfrac{1}{2}(\sigma_R + \sigma_L),$$

where σ_R and σ_L are the fractional energy fluctuations measured by summing the left and the right readout, respectively, of all calorimeter sections. For the case of configuration 2, these left and right readout calorimeters are simply the two interleaved calorimeters described in section 3.

Some remarks to the values contained in tables 3 and 4 are listed below.

1) All fluctuations scale with $\sqrt{E}$ as expected for compensating calorimeters. The small rise observed for σ_{sum} and σ_{side} is compatible with the known beam momentum spread of 1% and the small rise in σ_{dif} can be explained by an energy dependence in the beam spot width. These effects have been neglected in the averages.
2) σ_{sum} is almost identical for configurations 1 and 2. As expected, the total energy resolution can be recovered by summing the two interleaved calorimeters.
3) The e/h ratios are the same for both configurations, as expected. We note that the values given here are uncorrected for energy leakage.
4) In the case of configuration 1, σ_{sum} and σ_{side} are almost identical and much larger than σ_{dif} (see also fig. 8a) both for electrons and hadrons. In fact σ_{dif} does not vanish, due to photoelectron fluctuations.
5) In the case of configuration 2, σ_{dif} and σ_{side} are considerably increased, as expected (see fig. 8b). In the case of electrons, we obtain $\sigma_{dif} \approx \sigma_{sum}$ and $\sigma_{side} \approx \sqrt{2}\,\sigma_{sum}$ thus the resolution is dominated by sampling fluctuations. In the case of hadrons $\sigma_{dif} < \sigma_{sum}$ and $\sigma_{side} < \sqrt{2}\,\sigma_{sum}$ thus intrinsic fluctuations are also present.

A first estimation of intrinsic and sampling fluctuations can be made using the formulae given in section 3:

$$\sigma_{samp} = \sigma_{side} \ominus \sigma_{sum} = 42.0\%/\sqrt{E} \text{ (lead case)} \quad \text{or}$$

$$32.5\%/\sqrt{E} \text{ (uranium case)}$$

$$\sigma_{intr} = \sigma_{sum} \ominus \sigma_{samp} = 11.3\%/\sqrt{E} \text{ (lead case)} \quad \text{or}$$

$$18.3\%/\sqrt{E} \text{ (uranium case)}$$

However, instrumental effects have to be taken into account. They are discussed in the next section.

7. Instrumental effects

We have considered three instrumental effects which might modify the simple estimation given above:
- photoelectron statistics,
- a finite beam size, and
- light attenuation in the scintillator.

The quantity σ_{dif}, which should vanish for configuration 1 in the case of a perfect calorimeter, has been used to extract information on instrumental effects.

The photoelectron fluctuations for the lead calorimeter have been determined from the width of the response to a light pulser [5] and the result is $\sigma_{pe} = 6.5\%/\sqrt{E}$. Since in the electron case the only additional contribution to σ_{dif} is the effect of the beam spot width, σ_{beam}, we obtain

$$\sigma_{beam} = \sigma_{dif} \ominus \sigma_{pe} = 8.6 \ominus 6.5 = 5.6\%/\sqrt{E}.$$

Therefore $\sigma_{beam} = 1\%$ at 30 GeV. This result is compati-

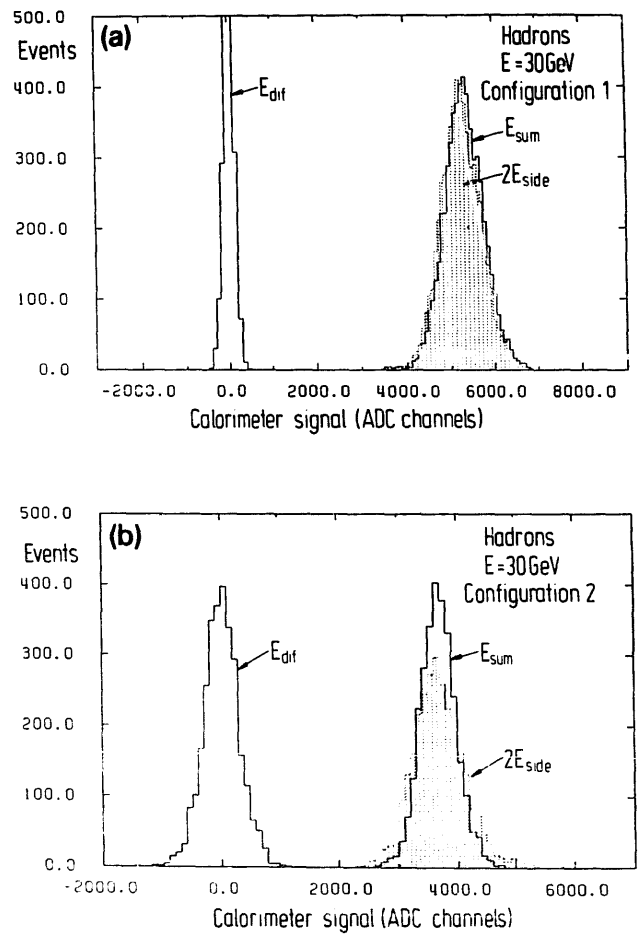

Fig. 8. (a) Pulse-height distributions for 30 GeV hadrons obtained with the lead-scintillator calorimeter in the case of configuration 1. (b) Pulse-height distributions for 30 GeV hadrons obtained with the lead-scintillator calorimeter in the case of configuration 2.

ble with a beam spot σ_d of 0.5 cm for $E = 30$ GeV (average energy) which yields

$$\sigma_{beam} = \frac{\sigma_d}{\lambda} \approx \frac{0.5}{60} \approx 0.8\%,$$

where λ is the effective light attenuation length in scintillator ($\lambda = 60$ cm for the lead calorimeter). In the case of the uranium calorimeter, no direct measurement of the light yield was available, but assuming a beam spot of 0.5 cm and an effective attenuation length of 100 cm [6] we obtain

$$\sigma_{pe} \approx 7.5\%/\sqrt{E}\,.$$

For the measurements performed with configuration 2, we have assumed the same beam spot widths and the following photoelectron fluctuations:

- lead calorimeter: $\sigma_{pe} = 7.0\%/\sqrt{E}$ (again measured with a light pulser),
- uranium calorimeter: $\sigma_{pe} = 10.5\%/\sqrt{E}$ (assuming a factor 2 for the loss in light yield).

For the lead calorimeter no significant loss in light yield is observed since the scintillator plates were covered by reflective teflon on the side which was not read out.

In the hadron case there is an additional contribution to σ_{dif}, namely σ_λ produced by transverse shower fluctuations in the scintillator. These shower fluctuations result in energy fluctuations due to the light attenuation length, whenever only one side of the scintillator plate is read out. We obtain this contribution in the following way (configuration 1):

$$\sigma_\lambda = \sigma_{dif}(\text{hadrons}) \ominus \sigma_{dif}(\text{electrons})$$
$$= 6.0\%/\sqrt{E} \text{ (lead)} \quad \text{and} \quad 8.3\%/\sqrt{E} \text{ (uranium)}.$$

In the case of the uranium calorimeter, σ_λ can be measured directly by making use of its transverse granularity in the vertical direction and weighting the energy deposited on each strip according to a simulated light attenuation in this direction. The measured energy is

$$E_0 = \sum_{i=1}^{12} E_i,$$

E_i being the energy deposited in each of the 12 transverse strips. For an assumed attenuation length $\lambda = 100$ cm in the vertical direction and a beam centered in strip 6, the energy is

$$E_\lambda = \sum_{i=1}^{12} E_i \, e^{(i-6)\Delta x/\lambda}$$

($\Delta x = 5$ cm is the strip height).

Due to transverse shower fluctuations, the quantity $E_{dif} = E_\lambda - E_0$ has a nonvanishing width ΔE_{dif} (see fig. 9 for 30 GeV hadrons). We obtain then

$$\sigma_\lambda = \frac{\Delta E_{dif}}{\langle E_0 \rangle} = \frac{7.0\%}{\sqrt{E}} \quad (E = 30 \text{ GeV}).$$

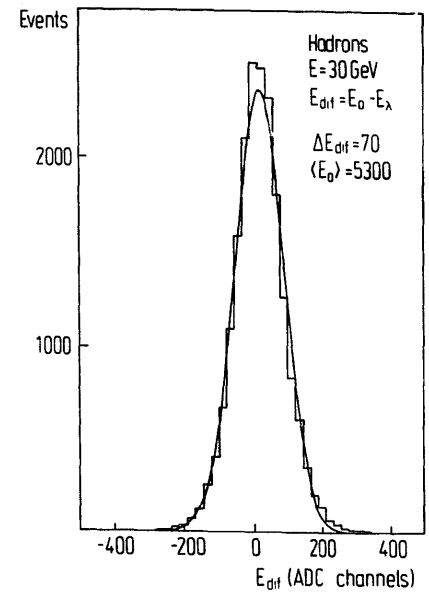

Fig. 9. E_{dif} for 30 GeV hadrons measured with the uranium–scintillator calorimeter in the case of configuration 1. As explained in the text, E_{dif} can be used to estimate the instrumental effects due to the scintillator attenuation length.

This value is in agreement with the previous one within errors. The same calculation performed for configuration 2 gives a similar value for σ_λ (7.4% instead of 7.0%), showing that transverse shower fluctuations are strongly correlated for the two interleaved calorimeters. We observe finally that although the attenuation length is smaller for the lead calorimeter (60 cm), the transverse horizontal readout is performed every 20 cm (instead of 60 cm), therefore we expect a smaller value of σ_λ.

A summary of these instrumental effects is given in tables 5a and 5b.

8. Results and discussion

Taking into account the instrumental effects mentioned in the previous section, we obtain the following

Table 5a
Instrumental effects for configuration 1 (30 GeV)

	$\sigma_{pe}\sqrt{E}$ [%]	$\sigma_{beam}\sqrt{E}$ [%]	$\sigma_\lambda\sqrt{E}$ [%]
Lead calorimeter	6.5	5.6	6.0
Uranium calorimeter	7.5	5.6	7.0

Table 5b
Instrumental effects for configuration 2 (30 GeV)

	$\sigma_{pe}\sqrt{E}$ [%]	$\sigma_{beam}\sqrt{E}$ [%]	$\sigma_\lambda\sqrt{E}$ [%]
Lead calorimeter	7.0	5.6	6.6
Uranium calorimeter	10.5	5.6	7.4

equations for the hadron shower fluctuations measured with configuration 2:

$$\sigma_{sum} = \sigma_{intr} \oplus \sigma_{samp} \oplus \sigma_{pe},$$

$$\sigma_{side} = \sigma_{intr} \oplus \sqrt{2}\,\sigma_{samp} \oplus \sqrt{2}\,\sigma_{pe} \oplus \sigma_{beam} \oplus \sigma_{\lambda},$$

$$\sigma_{dif} = \sigma_{samp} \oplus \sigma_{pe} \oplus \sigma_{beam} \oplus \sigma_{\lambda}.$$

This is an overconstrained system of three equations with two unknowns, σ_{intr} and σ_{samp} and the following consistency condition:

$$\sigma_{sum} \oplus \sigma_{dif} = \sigma_{side},$$

which is experimentally very well satisfied for both calorimeters. The intrinsic and sampling fluctuations for hadron showers obtained from the numbers of tables 3b, 4b and 5b are listed below:

- Lead calorimeter: $\sigma_{samp} = (41.2 \pm 0.9)\%/\sqrt{E}$ and $\sigma_{intr} = (13.4 \pm 4.7)\%/\sqrt{E}$,
- uranium calorimeter: $\sigma_{samp} = (31.1 \pm 0.9)\%/\sqrt{E}$ and $\sigma_{intr} = (20.4 \pm 2.4)\%/\sqrt{E}$.

For electron showers, we obtain by the same method ($\sigma_{\lambda} = 0$) the following result:

- lead calorimeter: $\sigma_{samp} = (23.5 \pm 0.5)\%/\sqrt{E}$ and $\sigma_{intr} = (0.3 \pm 5.1)\%/\sqrt{E}$,
- uranium calorimeter: $\sigma_{samp} = (16.5 \pm 0.5)\%/\sqrt{E}$ and $\sigma_{intr} = (2.2 \pm 4.8)\%/\sqrt{E}$.

We note that the uncertainty in the instrumental effects has no significant influence on the results. These results are given in tables 6a and 6b. No attempt has been made to correct for fluctuations in the energy leakage, which can only affect the intrinsic fluctuations. The sampling fluctuations for electrons are compatible with EGS calculations.

The following conclusions can be drawn.

1) The energy resolution for hadrons is dominated by sampling fluctuations for both calorimeters and particularly in the lead case where a coarse sampling was selected in order to achieve compensation. The sampling fluctuations are

$$\sigma_{samp} \approx 11.5\%\sqrt{\Delta\epsilon[\mathrm{MeV}]}\,/\sqrt{E[\mathrm{GeV}]},$$

where $\Delta\epsilon$ is the energy loss by mips per sampling layer as discussed in section 2. This value is slightly larger than a previously published one [12] of

$$\sigma_{samp} \approx 9\%\sqrt{\Delta\epsilon[\mathrm{MeV}]}\,/\sqrt{E[\mathrm{GeV}]}.$$

2) Sampling fluctuations for hadrons are larger than sampling fluctuations for electrons by a factor 2.
3) The measured intrinsic fluctuations are larger in uranium than in lead: $(20.4 \pm 2.4)\%/\sqrt{E}$ as compared to $(13.4 \pm 4.7)\%/\sqrt{E}$. The comparison is however made for calorimeters with very different sampling ratios: $R \approx 1$ for uranium, $R \approx 4$ for lead. Intrinsic fluctuations depend possibly on these ratios. The measured intrinsic fluctuations for uranium are compatible with a previously published value of $22\%/\sqrt{E}$ [12].

Table 6a
Results of the lead calorimeter ($\Delta\epsilon = 13.3$ MeV)

	$\sigma_{intr}\sqrt{E}$ [%]	$\sigma_{samp}\sqrt{E}$ [%]	$\sigma_{samp}\sqrt{E}/\sqrt{\Delta\epsilon}$ [%]
Hadrons	13.4±4.7	41.2±0.9	11.3±0.3
Electrons	0.3±5.1	23.5±0.5	6.4±0.2

Table 6b
Results of the uranium calorimeter ($\Delta\epsilon = 7.2$ MeV)

	$\sigma_{intr}\sqrt{E}$ [%]	$\sigma_{samp}\sqrt{E}$ [%]	$\sigma_{samp}\sqrt{E}/\sqrt{\Delta\epsilon}$ [%]
Hadrons	20.4±2.4	31.1±0.9	11.6±0.4
Electrons	2.2±4.8	16.5±0.5	6.1±0.2

9. Summary

We have measured the intrinsic and sampling fluctuations of two compensating sampling calorimeters for hadron showers in the energy range of 10–50 GeV by the method of the two interleaved calorimeters. These sampling calorimeters consisted of:

- scintillator plates (2.5 mm thick) sandwiched with lead plates (10 mm thick),
- scintillator plates (3.0 mm thick) sandwiched with uranium plates (3.2 mm thick).

We have found the following result for the sampling fluctuations:

$$\sigma_{samp} = (41.2 \pm 0.9)\%/\sqrt{E} \text{ (lead)} \quad \text{and}$$

$$\sigma_{samp} = (31.1 \pm 0.9)\%/\sqrt{E} \text{ (uranium)},$$

and for the intrinsic fluctuations:

$$\sigma_{intr} = (13.4 \pm 4.7)\%/\sqrt{E} \text{ (lead)} \quad \text{and}$$

$$\sigma_{intr} = (20.4 \pm 2.4)\%/\sqrt{E} \text{ (uranium)}.$$

The sampling fluctuations are described by the formula

$$\sigma_{samp} \approx 11.5\%\sqrt{\Delta\epsilon[\mathrm{MeV}]}\,/\sqrt{E[\mathrm{GeV}]},$$

where $\Delta\epsilon$ is the average energy loss of a minimum ionizing particle in one calorimeter layer. The intrinsic fluctuations for uranium are compatible with a previously published value of $22\%/\sqrt{E}$.

Acknowledgements

We gratefully acknowledge K. Westphal for technical support during the modification of the calorimeters. We are grateful for the hospitality extended to us during our stay at CERN and for the support of the CERN SPS-EA group during the setting up and running of the

experiment. We would also like to thank R. Wigmans for helpful discussions.

References

[1] J. Brau and T. Gabriel, Nucl. Intr. and Meth. A238 (1985) 489.
[2] H. Brückmann, U. Behrens, and B. Anders, DESY 86-155 (1986).
[3] R. Wigmans, Nucl. Instr. and Meth. A259 (1987) 389.
[4] T. Akesson et al., Nucl. Instr. and Meth. A241 (1985) 17; B. Anders et al., DESY 86–105; T. Akesson et al., Nucl. Instr. and Meth. A262 (1987) 243.
[5] E. Bernardi et al., Nucl. Instr. and Meth. A262 (1987) 229.
[6] G. d'Agostini et al., Nucl. Instr. and Meth. A274 (1989) 134.
[7] M. Abolins et al., Fermilab-Pub-89/38-E.
[8] K. Ankoviak et al., Nucl. Instr. and Meth. A279 (1989) 83.
[9] E. Borchi et al., Nucl. Instr. and Meth. A279 (1989) 57.
[10] R. Wigmans, The spaghetti calorimeter project at CERN, Proc. Workshop on Detectors at pp Colliders, Snowmass (1988).
[11] H. Tiecke, Nucl. Instr. and Meth. A277 (1989) 42.
[12] C.W. Fabjan, Calorimetry in high energy physics, CERN-EP/85-54, Techniques and Concepts of High Energy Physics III, (Plenum, 1985).
[13] C.W. Fabjan et al., Nucl. Instr. and Meth. 141 (1977) 61.
[14] W.R. Nelson, H. Hirayama and D.W.O. Rogers, SLAC 265 (1985).